Thermomechanical relaxation and different water states in cottonseed protein derived bioplastics†

H.-B. Yue,*[abc] J. P. Fernandez-Blazquez,[b] P. S. Shuttleworth,*[d] Y.-D. Cui[a] and G. Ellis[d]

Thermomechanical relaxation events and different water states in cottonseed protein bioplastics are presented whilst investigating the effects of aldehyde cross-linking agents. Thermomechanical relaxation of cottonseed protein bioplastics associated with protein denaturation, moisture absorption and broad glass transitions (T_g) were observed from DSC and DMA measurements. It was shown that variation of the aldehyde influences the storage modulus at very low temperature (below T_g). From measurements of the water fusion point, enthalpy, vaporisation, and weight loss, three water states in the water-absorbed bioplastics are suggested; namely strongly-bound-to-polymer, weakly-bound-to-polymer and bulk-like water. The water content and unreacted cross-linking agents are influential factors in controlling formation of the different water states, whilst the selection of different aldehydes was found to be negligible. These results could be valuable for adjusting the thermomechanical relaxations of protein based bioplastics, and tailoring their properties in wet environments.

Introduction

Protein based bioplastics (PBBs) have attracted renewed attention over the last few decades due to increased awareness of the environmental impact of petroleum based polymers and the rising costs of raw materials. Biopolymer alternatives from both plant and animal proteins such as soy, corn zein, wheat gluten, sunflower, peanut, cottonseed, milk casein, fish gelatin, feather quill, and serum albumin, have been studied as biofilm-forming agents.[1–9] Furthermore, bioplastics made from underutilised waste protein sources have emerged as a new family of renewable and sustainable plastics, known as "Second Generation Bioplastics"[3,10–12] owing to their low cost, availability and biodegradability.

There have been numerous studies focused on the thermal relaxation behaviour of PBBs macromolecular chains at temperatures ranging from −50 to 250 °C.[6,13,14] Within this temperature range many of the thermal induced events such as protein denaturing, ice-melting and, to some extent, degradation can be detected. Above this temperature range, most PBBs degrade. On the contrary, thermal events involving local chain motions often take place at lower temperatures than described, and as such have rarely been reported. Examples are the secondary gamma (T_γ) or beta (T_β) transitions[15] associated with localized bond/side chain movement (bending and stretching) as the polymer warms and expands from a tightly compressed solid state, or transitions where whole side chains and localized groups of the main chain begin to absorb sufficient energy to move and where the material develops toughness. The thermal complexity of these systems is of interest, and is highlighted by the fact that there is no consensus on the glass transition (T_g) temperatures for PBBs, partially due to the fact that these complex thermal relaxations are often overlapped. For example, in soy protein–glycerol–water bioplastic systems Chen *et al.*[16] identified three glass transition temperatures (T_{g1}, T_{g2} and T_{g3}) by differential scanning calorimetry (DSC), corresponding to glycerol-rich, protein-rich and protein–water domains. Thus, the first objective of this study was to investigate the thermal relaxation behaviour of gland-less cottonseed protein bioplastics (CPBs) previously prepared by hot-compression molding,[17] with a view to differentiate the sub-T_g transitions from the primary protein denaturation event through dynamic mechanical analysis (DMA) and DSC measurements.

PBBs are hydrophilic in nature and, as such, are sensitive to moisture, which in turn can deteriorate their mechanical properties. This effect is general for all kinds of PBBs[1,6,18] from a variety of protein resources. Cross-linking has been found not only to be an effective way to improve their mechanical and thermal stability properties, but is also reported to be effective in reducing water absorption, limiting the free space available

[a]*State Key Laboratory of Solidification Processing, School of Materials Science and Engineering, Northwestern Polytechnical University, Xi'an, Shaanxi 710072, China. E-mail: hangbo.yue@imdea.org*

[b]*IMDEA Materials Institute, c/Eric Kandel 2, Getafe 28906, Madrid, Spain*

[c]*E.T.S.I. Industriales, Universidad Politécnica de Madrid, c/José Gutiérrez Abascal 2, 28006 Madrid, Spain*

[d]*Department of Polymer Physics, Elastomers and Energy, Institute of Polymer Science and Technology (ICTP-CSIC), Juan de la Cierva 3, 28006 Madrid, Spain. E-mail: peter@ictp.csic.es*

for water molecules to penetrate the protein plastic.[12] Aldehydes such as formaldehyde, glyoxal, and glutaraldehyde that can readily react with the amine groups in proteins have been reported as the most commonly used cross-linking agents for PBBs since the 1930s when the first protein biofilm was formed by cross-linking casein protein with formaldehyde.[19] Cross-linking treatments using different aldehydes can also bring about different water transport behaviours in PBBs, which is mainly ascribed to the differences in cross-linking efficiency of the aldehydes,[20,21] and assumed to be associated with the presence of water in different states. Interestingly, water molecules in hydrophilic polymers behave differently to water in its free state (in bulk) and can be divided into three different conditions: (1) free water, (2) freezable bound water and (3) non-freezable bound water.[22,23] While the majority of the work in this area has been focused on conventional polymer systems in aqueous media, the question of how molecular water exists when absorbed in PBBs and what factors are predominant for adjusting the water states remains unanswered.

Experimental

Materials

Glandless cottonseed flour was obtained from Cotton-unis Biotech Co. Ltd., China, with a protein content of 57.2 wt% obtained using the Kjeldahl method for determining nitrogen with a conversion factor of 6.25. Urea, glycerol, formaldehyde (FA) (400 g L^{-1} or 40% v/v), glyoxal (GX) (400 g L^{-1} or 31% v/v), and glutaraldehyde (GA) (500 g L^{-1} or 47% v/v) were purchased from Guangzhou Chemical Reagent Factory, and used without further treatment. Note that formaldehyde, glyoxal, or glutaraldehyde in water is often present in a hydrated state, namely a methylene glycol hydrate $CH_2(OH)_2$ for formaldehyde,[22] monomer hydrates (OCHCHO, $OCHCH(OH)_2$, $(HO)_2CHCH(OH)_2$) or dioxolanes $[(HO)CH]_2O_2CHCHO$ for glyoxal,[23] and different hydrate species (hemihydrate, dihydrate, and cyclic hemiacetal) for glutaraldehyde.[24]

Preparation of cottonseed protein bioplastics

The preparation of CPBs has been previously reported.[17] Initially, cottonseed protein was denatured using a urea solution, which was then adjusted to pH 11 ± 0.1 with 1 N NaOH solution, the aldehyde cross-linking agent added, and the mixture vacuum-dried for 10 h at 80 °C. Homogeneous addition of glycerol to the dried solid was ensured using both a high-speed mixer and a three roller mill. This mixture was then further conditioned in a desiccator at room temperature for 24 hours and then hot pressed at 20 MPa, 130 °C for 5 minutes. The resultant CPB products were stored in a desiccator until characterized.

For simplicity, the modified CPBs are denominated CP-FA, CP-GX, and CP-GA representing the sample made from CP cross-linked with formaldehyde, glyoxal, and glutaraldehyde, respectively. The CPB with no cross-linking agent added and fabricated using the same procedure was denominated CP-0CL.

Measurements on different water states

To identify the different water states within the CPBs after water absorption, differential scanning calorimetry (DSC) measurements were carried out under nitrogen atmosphere using a TA Instruments Q200 DSC equipped with a cooling pump. Prior to testing, each specimen was weighed (~5–6 mg) into an aluminium (Al) pan, and a known amount of water added using a micro-syringe. The pan was then hermetically sealed with an Al cover and conditioned for 24 h at room temperature in order to allow the water absorption states to equilibrate. The water content ω_{H_2O} was calculated by:

$$\omega_{H_2O}(\%) = \frac{W_{H_2O}^{add}}{W_{CPBs}} \times 100 \quad (1)$$

where $W_{H_2O}^{add}$ and W_{CPBs} denote the weight of water added and that of the CPBs tested, respectively. W_{CPBs} is the total mass of the sample, *i.e.*, the sum of the dried sample and the water added. The samples conditioned were first equilibrated at −80 °C for 10 min, and then heated at a rate of 10 °C min^{-1} to 50 °C, with the procedure repeated three times to verify reproducibility. After the DSC measurements, all the hermetic Al pans were weighed to ensure no loss of sample weight during the experiment.

Free water is that containing both freezable bulk water and freezable water that is weakly bound to the polymer, and whose weight percentage $\omega_{H_2O}^{free}$ is:

$$\omega_{H_2O}^{free}(\%) = \left(W_{H_2O}^{free} \Big/ W_{H_2O}^{add}\right) \times 100 \quad (2)$$

$$W_{H_2O}^{free} = \frac{\Delta H_{W_{CPBs}}}{\Delta H_{pure\ H_2O}} \times W_{CPBs} \quad (3)$$

where $W_{H_2O}^{free}$ is the weight of the free water component within the bulk sample, obtained by multiplying the weight fraction of water (determined as $\Delta H_{W_{CPBs}}/\Delta H_{pure\ H_2O}$) with the total mass of the tested sample (W_{CPBs}). Here $\Delta H_{W_{CPBs}}$ is calculated by integrating the endothermic ice-melting peak, related to the total mass of the tested sample (sum of the dried sample and water added). It should be noted that it is not normalized with water mass, which is the case as shown in Table S1 and defined by eqn (S1).† $\Delta H_{pure\ H_2O}$ is the melting enthalpy of pure water, and calculated to be 365 J g^{-1} using distilled water as a reference for all samples. The weight percentage of non-free water $\omega_{H_2O}^{non\text{-}free}$, referring to non-freezable strongly-bound-to-polymer water, is obtained from the difference between the weight percentage of water added and that of free water. Providing that no endothermic peak is detected, the small amount of added water is considered both strongly bound to the polymer and non-freezable.

$$\omega_{H_2O}^{non\text{-}free}(\%) = \left(W_{H_2O}^{non\text{-}free} \Big/ W_{H_2O}^{add}\right) \times 100 \quad (4)$$

$$W_{H_2O}^{non\text{-}free} = W_{H_2O}^{add} - W_{H_2O}^{free} \quad (5)$$

Another series of samples after water absorption at two time intervals (30 min and 2 h) were measured using a TA

Instruments Q200 DSC calorimeter using the same protocol as before, except that the maximum temperature was 250 °C. In addition to the DSC measurements, the same specimens were measured on a TGA-50 thermo-gravimetric analyser (TA Instruments) at a heating rate of 10 °C min^{-1} from 25 to 250 °C, supplied with a 15 mL min^{-1} nitrogen flow.

Dynamic mechanical analysis

Thermal relaxations of the cross-linked bioplastics were carried out on a dynamic mechanical analyser (DMA Q800, TA Instruments) in tension mode with a preload force of 10 mN, displacement amplitude of 3.5 μm at 3, 7 and 10 Hz. Samples with dimensions 20 × 4.5 × 0.7 mm were heated from −140 to 180 °C at a heating rate of 1 °C min^{-1}.

Infrared spectroscopy

FTIR spectra of the raw CPB and CPBs cross-linked with different aldehydes were recorded using a Perkin-Elmer Spectrum One with a horizontal ATR accessory (Diamond/ZnSe crystal, $n = 2.4$). Further measurements were undertaken using a micro-ATR objective (Ge crystal, $n = 4.0$) in a Perkin-Elmer i-Series IMAGE infrared microscope coupled to a Spectrum 2000 FTIR spectrometer, where several spectra were measured from different positions on each sample. All spectra were recorded over the 4000–600 cm^{-1} frequency range, with a spectral resolution of 4 cm^{-1} accumulating 32 scans for each spectrum.

Results and discussion

Thermomechanical relaxation of CPBs

Complete denaturation of the unmodified cottonseed protein within the cross-linked CPBs matrices takes place at about 150 °C as the baseline increases from the minima, Fig. 1a, rather than at two temperatures characteristic of gossypin (11S) and congossypin (7S) globulin fractions as observed for other proteins, particularly soy.[25] It is also noted that the denaturation temperature (T_d) is similar for all the modified CPBs irrespective of the type of aldehyde cross-linking agent used. During denaturation of the cottonseed protein, multiple changes simultaneously occur involving hydrogen bonding, dipole–dipole, charge–charge, and hydrophobic interactions, due to the fact that the protein is comprised of a variety of different amino acid species. These interactions and further cross-linking reactions readily induce insoluble protein aggregation, which is normally accompanied by a low transitional energy[26] and thereby difficult to detect using DSC, similar to the sub-T_g transitions. Thus, dynamic mechanical analysis (DMA) was employed to detect thermomechanical relaxation of the cross-linked CPBs due to its better sensitivity to these types of thermal events. As shown in Fig. 1b, the denaturation temperature of CP can be clearly identified in the region $T_d = 120$ °C, corresponding to the α transition. Similar to the DSC results, cross-linking provokes little change in T_d. This suggests that the three aldehydes tested, formaldehyde (FA), glyoxal (GX) and glutaraldehyde (GA) generate a cross-linked network with a similar density, which is

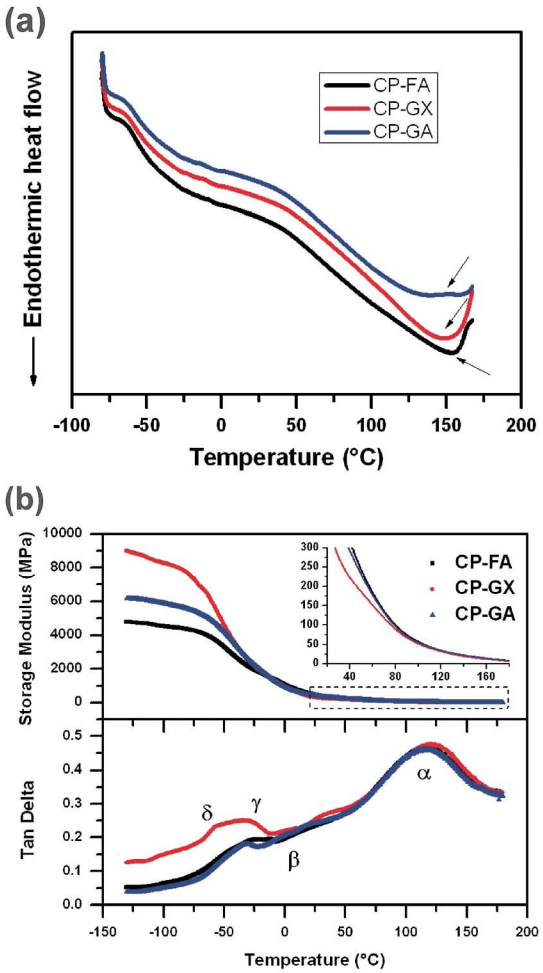

Fig. 1 DSC (a) and DMA (b) thermograms of the aldehyde cross-linked CP-FA, CP-GX and CP-GA CPBs. The temperatures marked in DSC curves indicate the T_d. Storage modulus and tan delta were obtained from DMA at 10 Hz with a heating rate of 1 °C min^{-1} from −140 to 180 °C. Inset is the enlarged plots marked by dashed rectangular.

nevertheless strongly dependent on the type of plasticizer.[27] Moreover, a small β transition peak at 0 °C (tan δ graph in Fig. 1b) is most likely associated with the absorption of moisture from air. A similar peak for soy protein–glycerol–water ternary systems was reported by Zhang *et al.*,[16] where it was assigned to the protein–water fraction, and found to occur at a higher relative humidity than 35%. A broad glass transition was observed from the storage modulus, E' profile shown in Fig. 1b, regardless of the type of cross-linking agent used. Correspondingly, two transitions denoted γ and δ were observed below 0 °C from the tan delta curves at ∼−25 °C and ∼−55 °C respectively. They are ascribed as glass transition temperatures from the large decrease in E' observed for all samples. PBBs have been known to have more than one T_g due to its heterogeneous nature.[13,16] For the sample CP-GX, a sub-T_g transitional behaviour is apparent at the very beginning of the E' decrement, around −100 °C, but is weaker in the other samples. In addition, there is a clear difference in the storage modulus of the samples at low temperatures, with the highest value (∼8500

MPa) found for CP-GX and the lowest for CP-FA (~4500 MPa) at −140 °C, Fig. 1b. However, a slightly lower value of E' for CP-GX after the glass transition may suggest a lower cross-linking density that would imply longer molecular chain length between crosslinks. This may lead to increased chain mobility that favours the formation of multiple intra- and intermolecular interactions, such as hydrogen bonding, that would contribute significantly to the mechanical reinforcement in the glassy state. Indeed, according to hydrogen bonding theories,[28] glyoxal is more likely to form hydrogen bonds with electronegative elements in the protein (O, S, N, *etc.*) than formaldehyde.

Different water states within CPBs

Fig. 2 shows the fusion, vaporisation and weight loss of the water used to dope the cross-linked CPBs as a function of temperature. In contrast to the dry CPBs, the samples after water absorption show a peak at 0 °C and 100 °C ascribed to ice melting and water vaporization (Fig. 2a). The enthalpy associated to these processes correlates with the amount of the water absorbed in the CPBs, with higher enthalpy values indicating more water absorbed. The same trend was found with respect to the weight loss of the CPBs at 100 °C from TGA measurements (Fig. 2b). For example, the CP-FA sample after 30 min and 2 h water absorption lost 24% and 41% of its original weight at 100 °C, respectively. Furthermore, DSC results (enthalpies of fusion and vaporisation, Table S1, in the ESI†) show that the CP-0CL sample absorbed more water than the cross-linked samples indicating that cross-linking leads to reduced water absorption.[17] The cross-linked bioplastics have a more compact, tightly bound structure that hinders water diffusion leading to lower water absorption. However, it is interesting to note that the ratio of water vaporisation enthalpy to enthalpy of fusion, $\Delta H_v/\Delta H_m$, is almost equivalent (10.0 ± 0.4sd) for all CPBs, and is higher than that of pure water (6.7) (Table S1, in the ESI†). This discrepancy suggests that water in the bioplastic networks behaves differently from its bulk-like characteristics. When compared with bulk-like water, water in the CPB systems may consist of either a higher content of evaporable water or a lower fraction of freezable water. To quantitatively differentiate between these different states of water, more detailed experiments on water content and its effects on the CPBs were undertaken.

The change in the fusion of water contained within the CPBs as a function of water concentration was measured using DSC, and the results are shown in Fig. 3. The heat of fusion for each sample changes considerably with increasing water content, from almost no endothermic response at a water content below 15% to a high value at water contents above 70%, showing a broad peak centred around 0 °C (Table S2, in the ESI†). In addition, increase in water content leads to an increase in the peak fusion temperature. Considering CP-FA as an example, the heat of fusion maximum temperature changes by 25 °C, from −24.9 to 0.1 °C, as the water content is increased from 19% to 75%. We propose that the formation of water layers on/within the biomass surface strongly depends on water content added; being strongly bound to CPBs at a lower concentration, both strongly and weakly bound at a slightly higher content,

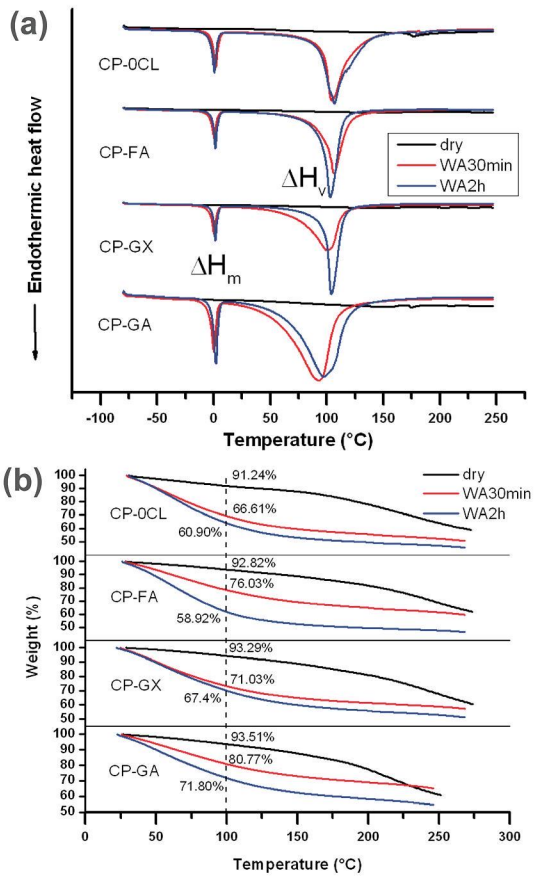

Fig. 2 DSC (a) and TGA (b) thermograms of CPBs dried, water absorbed for 30 min and 2 h, respectively. WA: water absorption; ΔH_m: enthalpy of fusion; ΔH_v: enthalpy of vaporisation.

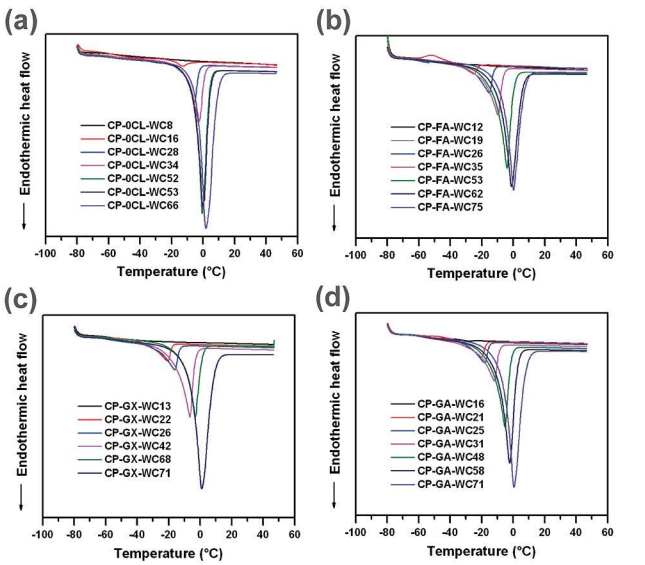

Fig. 3 DSC thermograms showing the change in enthalpy and peak fusion temperature of the CPBs with respect to water content (WC, %). (a) CP-0CL; (b) CP-FA; (c) CP-GX, and (d) CP-GA series.

and lastly, a ternary strongly to weakly bound to free system at an even higher water content (saturation).

The heat of fusion pattern shown in Fig. 3 suggests that the water contained within the CPBs structures can be subdivided into different states, *i.e.*, non-freezable water, free bulk-like water and freezable bound water, as reported for other hydrophilic polymers.[29,30] Different states of water in CPB networks can be attributed to the contribution of bonding strength or interactions (hydrogen bonds formed) between water and the polar groups on CPB polymer chains. Fig. 4 illustrates the bonding ability of CPB polymer chains with the water molecules, showing in part that strongly-bound-to-polymer water (SB2PW) could not freeze upon cooling, a fraction of freezable weakly-bound-to-polymer water (WB2PW) whose mobility is partially retarded, and an amount of freezable bulk-like water (BLW).

Weight fractions of water in different states within the CPBs can be readily calculated according to eqn (2)–(5) and are shown in Fig. 5 and further detailed in Table S2 of the ESI.† With increasing water content within the CPBs network, it is believed that water adopts at least three different states. At lower concentrations, it is present in the SB2PW state where it is strongly connected to protein polymer chains, and thus cannot freeze, as demonstrated in Fig. 3 where no endothermic heat flow is detected. Next, the CPB system containing a water content above a certain threshold appears as WB2PW, the intermediate state, suggesting a boundary where water molecules whose mobility is partially retarded could not sufficiently interact with the polymer chains to prevent the state of fusion, yet are able to crystallize as indicated in Fig. 3, from which increasing in water content leads to increases in both the peak fusion temperature (from ~−20 to ~0 °C) and the enthalpy of the endothermic heat flow. Lastly, excess water or BLW, evidenced by a broad peak centred at 0 °C in Fig. 3, is free of interactions with the protein chains, and is the predominant fraction at higher water contents (Fig. 5). For example, more than 60% of free water was found in all CPBs containing 40% water content, above which the weight fraction of free and non-free water reaches a plateau. It is likely that there exists another border, beyond which water is free of polymer interaction, behaving like BLW. Similarly, two critical thresholds to form different states of water in poly(vinyl alcohol) hydrogels have been reported.[31]

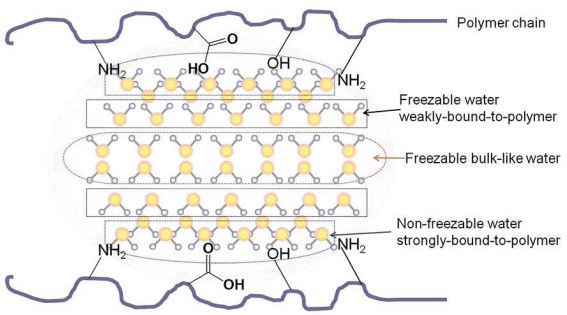

Fig. 4 Schematic of CPBs polymer chains affinity to water molecules, illustrating the presence of different states of water: freezable bulk-like water, freezable and non-freezable bound-to-polymer water.

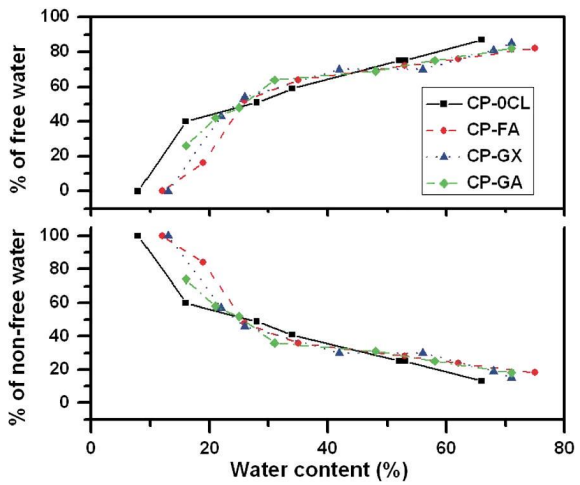

Fig. 5 The fractions of free and non-free water in the CPBs networks with different water content.

By evaluating the water transportation behaviour in CPBs, we have shown previously[17] that the cross-linked structures promote water diffusion and permeability, whereas the non-crosslinked polymer structure favours chemical interactions. Compared with the cross-linked CPBs (CP-FA, CP-GX and CP-GA), the CP-0CL sample presented the highest fraction of free water and lowest percentage of non-free water (Fig. 5). This implication is supported by the differences in the melting temperature (T_m) of water in the CPBs networks, as shown in Fig. S1† where water within the CP-0CL network melts at a higher temperature compared to all the other cross-linked CPBs.

With respect to the cross-linked samples (CP-FA, CP-GX and CP-GA), it is very difficult to differentiate the various water states (Fig. 5 and S1†), albeit between each aldehydes differences exist in factors such as cross-linking efficiency[21] and polarity, and each cross-links the protein chains in a different manner. Specifically, formaldehyde forms methylene bridges with protein molecules (Scheme S1a, in the ESI†) to create the cross-linked structure, whilst glutaraldehyde or glutaraldehyde polymer and glyoxal crosslink the protein molecules *via* Maillard-driven generation of the imine covalent bonds (Scheme S1b, in the ESI†), a diversity that is partially inferred in the infrared data.

Regardless of the functional group contribution from the protein chains, it is believed that hydrogen bonding between water and cross-linking agents within CPBs is strong enough to form the SB2PW. In the FTIR spectra in Fig. 6, in addition to the amide stretching bands (3218 cm^{-1}) and cross-link generated imine bands (1651 cm^{-1}), characteristic absorption bands of the aldehyde groups appear at around 1697 cm^{-1}, probably indicating the presence of un-reacted, or partially reacted, cross-linking agents distributed with variable concentration in the CPBs networks. Whereas the bulk spectroscopic measurements in Fig. 6 show the cross-linked CPBs to have very similar spectral profiles, microscale heterogeneity in the distribution of the

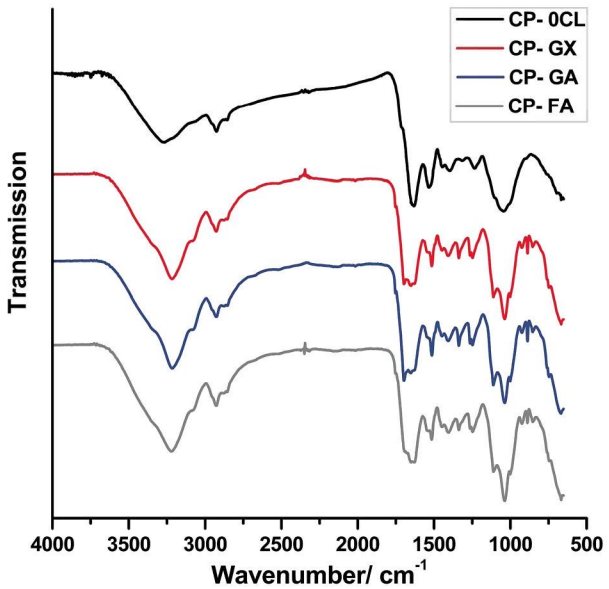

Fig. 6 ATR-FTIR spectra of CPBs with no cross-linking agent added (CP-0CL), and those cross-linked with different aldehydes (CP-FA, CP-GX and CP-GA).

components was observed in IR microspectroscopy measurements (see Fig. S2 of the ESI†). It is clear that an unequivocal verification of the nature and extent of the cross-linking reactions is difficult due to the spectral complexity of the systems. In particular, evidence for the formation of methylene bridges is severely limited as characteristic CH_2 bands are already present in the system.

It is important to point out that the higher fractions of non-freezable water found in all cross-linked CPBs (Fig. 5) should result from hydrogen bonding interactions between the remaining aldehydes and water molecules. Whilst the IR evidence does not provide clear evidence for the existence of different water states, the heterogeneous distribution of aldehyde clearly affects the uptake of water (Fig. S3, ESI†), and must affect the bound state it will adopt. Further work is required, perhaps employing spatially resolved infrared imaging microspectroscopy in a strictly controlled environment, to provide more insight into this network system in order to fully elucidate the nature of the localised cross-linking mechanisms.

Conclusion

Thermal mechanical relaxation and different water states in cottonseed protein bioplastics (CPBs) were investigated. According to DMA results, it was found that four different relaxation behaviours occurred in the cross-linked CPBs, namely protein denaturation (α relaxation), a weak β transition associated with moisture absorption, and glass transitions (γ and δ transitions). Different cross-linking agents have no obvious impacts on protein denaturation, but bring about a clear difference in storage modulus at a very low temperature. The experimental results based on the fusion of water, vaporisation and weight loss of all the water-absorbed bioplastics demonstrate that three different states of water are present within the sample. With increasing water content in the CPBs networks, water adopts three states: non-freezable strongly-bond-to-polymer water, freezable weakly-bond-to-polymer water, and freezable bulk-like water. In addition, the remaining un-reacted aldehyde in CPBs plays an important role in the formation of bound-to-polymer water, since they have a strong bonding strength with water as evidenced by infrared spectroscopy. However, different types of aldehyde as a cross-linking agent have a marginal impact on the creation of the different water states.

Acknowledgements

We thank financial supports from National Natural Science Foundation of China (Grant no. 20776164; 21176269), China Scholarship Council, "Marie Curie" Amarout Europe Programme, and PS gratefully acknowledges the Ministerio de Ciencia e Innovación for the concession of a Juan de la Cierva (JCI-2011-10836) contract. Lastly we thank the characterisation services of the ICTP-CSIC for their assistance with some of the measurements.

Notes and references

1 F. Song, D.-L. Tang, X.-L. Wang and Y.-Z. Wang, *Biomacromolecules*, 2011, **12**, 3369–3380.
2 F. Ayhllon-Meixueiro, C. Vaca-Garcia and F. Silvestre, *J. Agric. Food Chem.*, 2000, **48**, 3032–3036.
3 A. Gennadios, *Protein-Based Films and Coatings*, CRC Press, 2002.
4 M. C. Gómez-Guillén, M. Pérez-Mateos, J. Gómez-Estaca, E. López-Caballero, B. Giménez and P. Montero, *Trends Food Sci. Technol.*, 2009, **20**, 3–16.
5 H. Ture, M. Gallstedt, R. Kuktaite, E. Johansson and M. S. Hedenqvist, *Soft Matter*, 2011, **7**, 9416–9423.
6 H. Zhang and G. Mittal, *Environ. Prog. Sustainable Energy*, 2010, **29**, 203–220.
7 A. Ullah, T. Vasanthan, D. Bressler, A. L. Elias and J. Wu, *Biomacromolecules*, 2011, **12**, 3826–3832.
8 T. Mekonnen, P. Mussone, H. Khalil and D. Bressler, *J. Mater. Chem. A*, 2013, **1**, 13379–13398.
9 R. Mülhaupt, *Macromol. Chem. Phys.*, 2013, **214**, 159–174.
10 J. Scheller and U. Conrad, *Curr. Opin. Plant Biol.*, 2005, **8**, 188–196.
11 W. Zhao, R. Yang, Y. Zhang and L. Wu, *Green Chem.*, 2012, **14**, 3352–3360.
12 C. Verbeek and L. van den Berg, *Recent Pat. Mater. Sci.*, 2009, **2**, 171–189.
13 P. Chen and L. Zhang, *Macromol. Biosci.*, 2005, **5**, 237–245.
14 L. Zhang, P. Chen, J. Huang, G. Yang and L. Zheng, *J. Appl. Polym. Sci.*, 2003, **88**, 422–427.
15 K. P. Menard, *Dynamic mechanical analysis: a practical introduction*, CRC Press, 2008.
16 P. Chen, L. Zhang and F. Cao, *Macromol. Biosci.*, 2005, **5**, 872–880.

17 H. B. Yue, Y. D. Cui, P. S. Shuttleworth and J. H. Clark, *Green Chem.*, 2012, **14**, 2009–2016.
18 R. P. Wool and X. S. Sun, *Bio-Based Polymers and Composites*, Elsevier Academic Press, 2005.
19 E. Sutermeister and F. L. Browne, *Casein and its industrial applications*, Reinhold, New York, 1939.
20 P. Davis and B. E. Tabor, *J. Polym. Sci., Part A: Gen. Pap.*, 1963, **1**, 799–815.
21 D. Hopwood, *Histochem. Cell Biol.*, 1969, **17**, 151–161.
22 N. Matubayasi, S. Morooka, M. Nakahara and H. Takahashi, *J. Mol. Liq.*, 2007, **134**, 58–63.
23 E. B. Whipple, *J. Am. Chem. Soc.*, 1970, **92**, 7183–7186.
24 E. B. Whipple and M. Ruta, *J. Org. Chem.*, 1974, **39**, 1666–1668.
25 X. Mo and X. Sun, *J. Am. Oil Chem. Soc.*, 2001, **78**, 867–872.
26 J. W. Donovan and K. D. Ross, *Biochemistry*, 1973, **12**, 512–517.
27 J. K. Sears and J. R. Darby, in *The Technology of Plasticizers*, ed. J. K.Sears and J. R. Darby, Wiley, 1982, pp. 35–77.
28 J. Emsley, *Chem. Soc. Rev.*, 1980, **9**, 91–124.
29 Z. H. Ping, Q. T. Nguyen, S. M. Chen, J. Q. Zhou and Y. D. Ding, *Polymer*, 2001, **42**, 8461–8467.
30 J. Ostrowska-Czubenko and M. Gierszewska-Drużyńska, *Carbohydr. Polym.*, 2009, **77**, 590–598.
31 W. Li, F. Xue and R. Cheng, *Polymer*, 2005, **46**, 12026–12031.